PERGAMON

International Journal of Heat and Mass Transfer 43 (2000) 3539–3550

International Journal of HEAT and MASS TRANSFER

www.elsevier.com/locate/ijhmt

The collapse of vapor bubbles in a spatially non-uniform flow

Y. Hao, A. Prosperetti*, [1]

Department of Mechanical Engineering, The Johns Hopkins University, Baltimore, MD 21218, USA

Received 13 July 1999; received in revised form 10 December 1999

Abstract

Pressure gradients act differently on liquid particles and suspended bubbles and are, therefore, capable of inducing a relative motion between the phases even when no relative velocity initially exists. As a consequence of the enhanced heat transfer in the presence of convection, this fact may have a major impact on the evolution of a vapor bubble. The effect is particularly strong in the case of a collapsing bubble for which, due to the conservation of the system's impulse, the induced relative velocity tends to be magnified when the bubble volume shrinks. A practical application could be, for instance, the enhancement of the condensation rate of bubbles downstream of a heated region, thereby reducing the quality of a flowing liquid–vapor mixture. A simple model of the process, in which the bubble is assumed to be spherical and the flow potential, is developed in the paper.

Keywords: Vapor bubbles; Two phase flow; Boiling

1. Introduction

It has long been appreciated that convection has a major effect on the heat transfer processes that lead to the growth or collapse of vapor bubbles in a liquid [1–9]. In most of the previous studies devoted to this problem, the relative velocity between the bubble and the liquid was either held constant or allowed to respond to buoyancy according to the instantaneous bubble volume. While both models are relevant for situations of pool boiling, they are less applicable to many cases of flow boiling in which the pressure gradient that is responsible for the flow acts differently on the bubble and the liquid, with the consequence that a relative motion between the two develops. This relative motion can be responsible for a variety of intriguing effects with an ultimate bearing on the bubble growth or collapse. These processes are of even greater importance under microgravity conditions in which an imposed flow is often the only means available for bubble management.

In the present paper, we discuss a simplified model of such a process. We assume the bubble to remain spherical allowing it to adjust its velocity relative to the liquid according to the local pressure gradient. Added mass effects, of course, feature prominently in these phenomena as, for example, a small relative velocity acquired under the action of the pressure gradi-

* Corresponding author. Tel.: +1-410-516-8534; fax: +1-410-516-7254.

E-mail address: prosperetti@jhu.edu (A. Prosperetti).

[1] Also: Department of Applied Physics, Twente Institute of Mechanics, and Burgerscentrum, University of Twente, AE 7500 Enschede, The Netherlands.

0017-9310/00/$ - see front matter
PII: S0017-9310(99)00389-0

Nomenclature

A	cross-sectional area
c	speed of sound in liquid
C_D	drag coefficient
c_p	specific heat at constant pressure
c_s	vapor specific heat along the saturation line
D	thermal diffusivity
Ja	$= \rho_L c_L (T_{sat} - T_\infty)/\rho_{V,sat} L$, Jacob number
k	liquid thermal conductivity
ℓ	length scale of the pressure distribution, Eq. (14)
L	latent heat
p_b	liquid pressure at the bubble surface
P	ambient liquid pressure
Pe	$= 2U_B R(0)/D$, Péclet number
P_N	Legendre polynomial
r	radial coordinate measured from the bubble center
R	bubble radius
Re	Reynolds number
S_N	coefficients in the temperature expansion (17)
t_c	$= \pi R^2(0)/4Ja^2 D$, characteristic time
T_L	liquid temperature
T_S	liquid temperature at the bubble surface
T_{2K}	Chebyshev polynomials
$\mathbf{u}$	liquid local velocity around the bubble
U_B	bubble translational velocity
U_L	liquid velocity
V_R	translational velocity of the bubble relative to the liquid
We	$= \rho_L V_R^2 R(0)/\sigma$, Weber number
x	polar axis, direction of motion of the bubble
z	auxiliary spatial variable defined in Eq. (23)

Greek symbols

α	parameter in the velocity and pressure distributions, Eq. (14)
δ	parameter for the initial temperature distribution, Eq. (26)
θ	polar angle measured from the direction of the relative velocity of the bubble
μ	liquid viscosity
ρ	density
σ	surface tension coefficient
τ	characteristic time

Subscripts

L	liquid quantity
sat	evaluated according to the saturation relation
V	vapor quantity
∞	evaluated far upstream

ent that can be significantly amplified in the course of the collapse. In turn, the greater heat transfer due to this increased convection will promote a faster collapse. This phenomenon may find a useful practical application in enhancing the condensation rate of bubbles downstream of a boiling region.

Translating bubbles were the object of considerable interest up to the early 70s, when some experimental data and quite a number of approximate analytical studies and numerical computations were published. In recent times, there has been a resurgence of interest in the topic due to the availability of better numerical and experimental methods (see, e.g., Refs. [10,11]). Legendre et al. [11] present a very detailed study of the heat transfer processes around a variable-radius, translating spherical bubble. They solve the complete Navier–Stokes equations, rather than using a potential flow approximation as given here. However, they assume the translational velocity to be a constant. Reference [12] studies the response of a translating bubble to a time-varying pressure, and is therefore different from the present one which focuses on a spatially-varying pressure and the attendant "virtual buoyancy" effect on the bubble. Reference [10] presents data on the departure of vapor bubbles injected in a subcooled liquid through the base of the container and their subsequent collapse. Due to the experimental requirements of holography, these bubbles are relatively large and significantly distorted and, therefore, rather different from the ones studied here. A large number of studies have been devoted to the growth and detachment of bubbles in pool boiling or on a wall exposed to a flow (for recent representative examples, see, e.g., Refs. [13–15]). Again, this situation is different from the present one, in which we envisage a bubble that is convected by the flow in a region of spatially non-uniform pressure, and follow the subsequent motion and heat transfer processes.

The assumption of sphericity, although quite common in the literature, is, of course, questionable particularly in the case of rapid condensation in which conservation of the liquid impulse forces the formation of jet traversing the bubble in the direction of motion [16,17]. This circumstance invalidates our predictions in the last stages of the collapse. Nevertheless, in a liquid like water, millimeter-size bubbles are fairly spherical due to surface tension effects, and even if the later details of the motion are incorrect, one may expect that the trends that we find would be representative of real phenomena.

2. Mathematical formulation

With the assumption of a spherical shape, the vapor volume is simply characterized by its time-dependent radius $R(t)$, the evolution of which is governed by Keller's equation

$$\left(1-\frac{\dot R}{c}\right)R\ddot R+\frac{3}{2}\left(1-\frac{\dot R}{3c}\right)\dot R^2 = \frac{1}{\rho_{\rm L}}\left(1+\frac{\dot R}{c}+\frac{R}{c}\frac{\rm d}{{\rm d}t}\right)(p_{\rm b}-P). \tag{1}$$

Here dots denote time derivatives, $\rho_{\rm L}$ is the liquid density, $p_{\rm b}$ is the liquid pressure at the bubble surface, and P is the ambient pressure which, for the present purpose, can be regarded as the pressure at the location of the bubble in the absence of the bubble. In Eq. (1), the terms divided by the liquid speed of sound c represent a first-order correction for the effects of liquid compressibility. A case could be made for augmenting the pressure P by the liquid pressure averaged over the surface of the bubble, $-(1/4)\rho_{\rm L}V_{\rm R}^2$, where $V_{\rm R}$ is the relative velocity (see, e.g., Refs. [18,19]), but the effect is negligible for the situations considered here and is disregarded.

The bubble internal pressure is strongly dependent on the surface temperature that must be determined by solving the liquid energy equation

$$\frac{\partial T_{\rm L}}{\partial t}+\mathbf{u}\cdot\nabla T_{\rm L}=D_{\rm L}\nabla^2 T_{\rm L}, \tag{2}$$

where $T_{\rm L}$ is the liquid temperature and $D_{\rm L}$ the liquid thermal diffusivity; $\mathbf{u}$ is the liquid velocity field in the bubble rest frame. This Eq. (2) should be solved subject to the condition that, at $r=R(t)$, the liquid temperature equals the local bubble surface temperature $T_{\rm S}$. In principle, it would be necessary to allow for surface temperature non-uniformities, but it is well known that such effects are very small due to the rapidity with which local processes of evaporation and condensation can erase such temperature differences. Hence, we assume that $T_{\rm S}$ is uniform over the bubble surface. The approximation of a spatially uniform pressure in the bubble is well justified when, as here, the vapor velocity is small with respect to the speed of sound [20]. Since, under the same conditions, the phase change processes occurring at the interface are slow enough for thermodynamic equilibrium conditions to prevail (see, e.g., Ref. [21]), the bubble internal pressure can be taken equal to the saturation pressure $p_{\rm sat}(T_{\rm S})$ at the instantaneous bubble surface temperature $T_{\rm S}$. The liquid pressure just outside the bubble surface, $p_{\rm b}$, is therefore related to the bubble internal pressure by the normal stress condition

$$p_{\rm sat}(T_{\rm S})=p_{\rm b}+\frac{2\sigma}{R}+4\mu_{\rm L}\frac{\dot R}{R}, \tag{3}$$

where σ is the surface tension coefficient and $\mu_{\rm L}$ the liquid viscosity. It is well known that viscous effects vanish identically in the momentum equation of an incompressible fluid in irrotational motion even when, as here, they give a non-zero contribution to the normal stress boundary condition.

A second condition to impose on the solution of the energy equation is conservation of energy at the bubble surface which is expressed by

$$\mathbf{n}\cdot(k_{\rm V}\nabla T_{\rm V}-k_{\rm L}\nabla T_{\rm L})=L\dot m, \tag{4}$$

where k is the thermal conductivity, L the latent heat, $\dot m$ the local mass flux, and $\mathbf{n}$ the unit normal. In a previous study [22], where we allowed a non-uniform temperature distribution in the vapor under conditions of spherical symmetry, it was shown that the vapor temperature can be considered approximately uniform provided that the parameter $\sqrt{D_V\tau}/R(0)$ (where $D_{\rm V}$ is the vapor thermal diffusivity and τ a characteristic time scale of the problem) is not too small. Here, we can estimate τ by using the time scale introduced in Ref. [3],

$$t_{\rm c}=\frac{\pi}{4Ja^2}\frac{R^2(0)}{D_{\rm L}}, \tag{5}$$

where Ja is the Jacob number defined by

$$Ja=\frac{\rho_{\rm L}c_{\rm pL}(T_{\rm sat}-T_\infty)}{\rho_{\rm V,\,sat}L}, \tag{6}$$

with $c_{\rm pL}$ the liquid specific heat and $T_{\rm sat}$ and $\rho_{\rm V,\,sat}$ the saturation values at the ambient pressure P_∞. Physically, $t_{\rm c}$ represents the order of magnitude of the time necessary to condense the bubble. With this choice we find

$$\frac{\sqrt{D_{\rm V}t_{\rm c}}}{R(0)}=\frac{1}{Ja}\sqrt{\frac{\pi}{4}\frac{D_{\rm V}}{D_{\rm L}}}. \tag{7}$$

For the liquids we consider $D_{\rm V}/D_{\rm L}\sim 10^2$–$10^3$ and Ja is of the order of 10. The condition is then satisfied and we deduce that the vapor temperature is very nearly uniform in the bubble, with the consequence that the vapor heat flux term in Eq. (4) is negligible. Averaging over the bubble surface (indicated by an overline), we can then impose the condition

$$4\pi R^2k_{\rm L}\left.\overline{\frac{\partial T}{\partial r}}\right|_{r=R(t)}=L\frac{\rm d}{{\rm d}t}\left(\frac{4}{3}\pi R^3\rho_{\rm V}\right)+\frac{4}{3}\pi R^3\rho_{\rm V}c_{\rm s}\frac{{\rm d}T_{\rm S}}{{\rm d}t}, \tag{8}$$

where $c_{\rm s}=c_{\rm pV}-L/T_{\rm S}$ (with $c_{\rm pV}$ the vapor specific heat at constant pressure) is the thermal heat capacity along

the saturation line, and ρ_V the saturated vapor density. The derivation of this equation from the energy equation in the gas and Eq. (4) is not entirely straightforward and is given in full in Ref. [22]. Even though the last term is often omitted in the literature, as it is mostly significant only for high rates of change of the surface temperature (as would prevail in an acoustic field or toward the end of a violent collapse), we retain it here for greater accuracy.

Non-condensible gases inside the bubble would be dependent on liquid preparation and the actual experimental conditions, and will be neglected here for simplicity and in order to limit the number of parameters.

With the neglect of viscosity, we approximate the liquid velocity field by the potential flow around a translating and collapsing or expanding sphere and write

$$\mathbf{u} = \nabla\left[-\frac{R^2\dot{R}}{r} + V_R r\left(1 + \frac{R^3}{2r^3}\right)\cos\theta\right], \tag{9}$$

where

$$V_R = U_B - U_L, \tag{10}$$

is the relative velocity of the bubble with respect to the liquid given by the difference of U_B and U_L, the bubble and liquid velocities in the laboratory frame. Here, we assume that the motion is rectilinear,θ is the polar angle measured from the direction of the relative velocity, and r is the distance from the bubble center. In order to determine V_R, we balance the added mass force against pressure gradient and drag to find (see, e.g., Refs. [17,23–26])

$$\frac{1}{2}\rho_L\left[\frac{4}{3}\pi R^3\left(\frac{dU_B}{dt} - U_L\frac{dU_L}{dx}\right) + V_R\frac{d}{dt}\left(\frac{4}{3}\pi R^3\right)\right] = -\frac{4}{3}\pi R^3\frac{dP}{dx} - C_D\pi R^2\frac{1}{2}\rho_L|V_R|V_R. \tag{11}$$

The terms in the left-hand side are the rate of change of the system impulse and represent the effect of the added mass interaction. The first term in the right-hand side (which can equivalently be written in terms of the liquid acceleration in place of the pressure gradient on the basis of the momentum equation) is sometimes referred to as "virtual buoyancy" because, if dP/dx is replaced by $\rho_L g$, one has a standard form of the equation of motion for a bubble in the gravitational field (see, e.g., Refs. [2,26]). The use of dP/dx to model the imposed pressure gradient which determines the ambient flow in which the bubble is immersed is justified when the characteristic length scale for variations of P is larger than the bubble radius, which is not a very stringent assumption. The argument can be outlined as follows (see, e.g., Ref. [27]). The pressure field surrounding a bubble in a flow can be approximately subdivided into a component p_s with a length scale comparable with the bubble radius (responsible for the added mass effect), and another component with a much slower spatial variation. One may vaguely refer to this quantity as the pressure at the bubble position in the absence of the bubble, which provides a justification for identifying it with the liquid pressure P. The force on the bubble due to this pressure component is

$$\mathbf{F}_p = -\int_S \mathbf{n}\cdot P(\mathbf{x}, t)\,dS, \tag{12}$$

where the integration is over the bubble surface, with outward unit normal $\mathbf{n}$. If we set $x = x_C + r$, where x_C is the bubble center, and carry out a Taylor series expansion of P, we immediately find $\mathbf{F}_p \simeq -V\nabla P$ as in Eq. (11), with V the bubble volume.

The last term in the right-hand side of Eq. (11) represents the drag force, with a drag coefficient C_D, for which many different expressions exist in the literature. Since, here, we use a potential flow approximation, it is appropriate to take the Levich form as corrected by Moore [28]

$$C_D = \frac{48}{Re}\left(1 - \frac{2.211}{Re^{0.5}}\right), \tag{13}$$

where the Reynolds number Re equals $2V_R R\rho_L/\mu$. The first term is the well-known boundary layer result derived by Levich [29] (see also Ref. [30]), and the second is term the correction due to Moore. Magnaudet and Legendre [26] have recently pointed out the limitations of drag estimates based on the assumption of a constant bubble radius but, at the same time, they show that the form (13) is fairly accurate at relatively high Reynolds and Jacob numbers, which are the cases studied here. In any event, for the cases we consider, the effects of drag are small as we have confirmed by using other drag relations and also by setting the drag to zero. Hence, the precise form of the drag relation that we use is not a matter of great concern.

The purpose of this paper is to point out the effect of pressure gradients in inducing a relative velocity between the bubble and the liquid and, therefore, an increase in the heat exchange rate between the two. For this purpose, it is useful to have a pressure field characterized by two parameters, one measuring the magnitude of the pressure change and the other one the spatial scale of the pressure variation. To derive one such parameterization, we form the mental picture of a uniform flow along the axis of a converging or diverging duct with a local cross-sectional area given by

$$\frac{A(x)}{A_\infty} = \frac{1+\alpha\tanh(x/\ell)}{1-\alpha}, \tag{14}$$

with A_∞, α, ℓ suitable constants. With the assumption of quasi-one-dimensional flow, we then have

$$\frac{\mathrm{d}P}{\mathrm{d}x} = -\rho_\mathrm{L} U_\mathrm{L} \frac{\mathrm{d}U_\mathrm{L}}{\mathrm{d}x}. \tag{15}$$

We stress that we do not intend this to be a model for the actual behavior of a vapor bubble in a variable-area duct, for which one should address the possibility of flow separation when $\mathrm{d}A/\mathrm{d}x > 0$, the effects of viscosity, turbulence, etc. Rather, this is a convenient two-parameter pressure field that enables us to point out a general tendency of bubble–liquid heat exchange in flows with pressure gradients.

Since the flow in which the bubble is immersed varies relatively slowly over the spatial scale of the bubble, as noted before, it is appropriate to take as the ambient pressure P, appearing in the Keller equation (1), the value of P given by Eq. (15) evaluated at the position of the bubble center. Integration of Eq. (15) gives

$$P = P_\infty - \frac{1}{2}\rho_\mathrm{L}\left(U_\mathrm{L}^2 - U_\infty^2\right), \tag{16}$$

where P_∞, U_∞ are the liquid pressure and velocity far upstream of the region where the pressure gradient is appreciable.

3. Numerical method

In order to solve the energy equation (2), we expand the liquid temperature T_L in a Legendre polynomial series as

$$T_\mathrm{L} = T_\infty + \sum_{N=0}^{\infty} S_N(r,t) P_N(\cos\theta), \tag{17}$$

substitute into Eq. (2), and take scalar products with the generic Legendre polynomial to find

$$\begin{aligned}
&\frac{\partial S_N}{\partial t} + \frac{R^2\dot{R}}{r^2}\frac{\partial S_N}{\partial r} + V_R\left(1-\frac{R^3}{r^3}\right)\\
&\quad\times\left(\frac{N}{2N-1}\frac{\partial S_{N-1}}{\partial r} + \frac{N+1}{2N+3}\frac{\partial S_{N+1}}{\partial r}\right)\\
&\quad+\frac{1}{r}V_R\left(1+\frac{R^3}{2r^3}\right)\left[-\frac{N(N-1)}{2N-1}S_{N-1}\right.\\
&\quad\left.+\frac{(N+1)(N+2)}{2N+3}S_{N+1}\right] = \frac{D_\mathrm{L}}{r^2}\left[\frac{\partial}{\partial r}\left(r^2\frac{\partial S_N}{\partial r}\right)\right.\\
&\quad\left.-N(N+1)S_N\right].
\end{aligned} \tag{18}$$

In practice, we truncate the expansion (17) to a maximum number of terms M; the component S_{M+1} that would arise in this equation is disregarded. From the continuity of temperature at the bubble surface, we deduce

$$S_0(R(t),t) = T_\mathrm{S}(t) - T_\infty, \quad S_K(R(t),t) = 0 \quad \text{for} \quad K = 1,2,\ldots,M. \tag{19}$$

The interface energy balance (8) gives instead

$$4\pi R^2 k_\mathrm{L}\left.\frac{\partial S_0}{\partial r}\right|_{r=R(t)} = L\frac{\mathrm{d}}{\mathrm{d}t}\left(\frac{4}{3}\pi R^3\rho_\mathrm{V}\right) + \frac{4}{3}\pi R^3\rho_\mathrm{V}C_\mathrm{s}\frac{\mathrm{d}T_\mathrm{S}}{\mathrm{d}t}. \tag{20}$$

Far from the bubble, we require that $T\to T_\infty$, and therefore

$$S_0\to T_\infty, \quad S_K\to 0 \quad \text{for} \quad K = 1,2,\ldots,M, \tag{21}$$

as $r\to\infty$.

Since, for $K\geq 1$, S_K is required to vanish at the bubble surface, no condition analogous to Eq. (20) is required. If needed, the local mass flux at the bubble surface could be obtained from Eq. (4) and the calculated values of $\partial S_K/\partial r$.

Eq. (18), written for $N = 0,1,\ldots,M$, constitute a system of coupled partial differential equations that we solve by a collocation method which extends the one used in our previous work [22]. We expand each S_N in a series of Chebyshev polynomials

$$S_N = \sum_{K=0}^{J} a_{NK}(t) T_{2K}(z), \tag{22}$$

where we have introduced the new spatial variable

$$z = \frac{m}{m+r-R(t)}, \tag{23}$$

where $m = \eta\sqrt{D\tau}$ is taken to be a multiple η of the thermal penetration depth in the liquid $\sqrt{D\tau}$. We take $\tau = t_\mathrm{c}$ defined in Eq. (5) whenever T_∞ is not too close to $T_\mathrm{sat}(P_\infty)$. For the other cases, we adjust τ by trial and error to have an accurate time resolution; the parameter η is typically taken to be 10. The variable z maps the domain $R(t)\leq r < \infty$ exterior to the bubble to the fixed domain $1\geq z > 0$. In Eq. (22), we use only the even Chebyshev polynomials T_{2K} to ensure that $\partial S_N/\partial r\to 0$ as $r\to\infty$.

For each S_N, the expansion (22) is substituted into Eq. (18) and the resulting expressions evaluated at the $J-1$ collocation points

$$z_j = \cos\frac{\pi j}{2J}, \quad j = 1,2,\ldots,J-1. \tag{24}$$

At $r = R(t)$ (i.e., $z = 1, j = 0$), we impose the interface boundary conditions (19) and (20), and for $r \to \infty$ (i.e., $z = 0, j = J$), the conditions (21). In this way, a system of ordinary differential equations sufficient for the determination of the coefficients $a_{NK}(t)$ is generated.

The validation of the method and a few additional details can be found in Ref. [22]. For the present study, we have conducted several preliminary tests to determine the number of terms sufficient to ensure converged results. We found that retaining eight terms in the Legendre polynomial expansion (17) and 16–32 terms in the Chebyshev expansion (22) resulted in a sufficient accuracy, except perhaps in the very last stages of the collapse when the relative velocity is large. Since our model is not expected to be accurate during this phase of the motion where one would expect significant departures from the spherical shape, errors of a few percent are of no great concern and we made no effort to correct them.

4. Results

In order to validate our code, we have compared our results with those of Wittke and Chao [4] for a bubble condensing while stationary or translating at constant velocity. A typical case is illustrated in Fig. 1a, to be compared with Fig. 10b of Wittke and Chao's paper; the results of these authors are shown by the circles. Here, the dotted line is for a stationary bubble and the dashed line for a constant bubble velocity corresponding to a Péclet number

$$Pe = \frac{2U_B R(0)}{D_L}, \tag{25}$$

of 1495; for both cases, the Jacob number is $Ja = 10$. In water at 1 atm (101.33 kPa), these values of Pe and Ja correspond to a subcooling of 3.35 K, $R(0) = 1$ mm, and a bubble velocity of 0.127 m/s. The solid line shows the result when the bubble velocity varies in time according to Eq. (11) starting from 0.127 m/s. Following Wittke and Chao, in this figure, time is expressed in units of t_c defined in Eq. (5) which, again for the case of water mentioned before, equals 46.2 ms. As in Wittke and Chao's paper, at $t = 0$, the bubble surface is at the saturation temperature, while $T = T_\infty$ elsewhere. In all the calculations that follow (except for Fig. 4), however, we take $T(R(0), 0) = T_\infty$.

A close inspection of our results reveals a slight rebound in the early stages of the collapse that is absent from Wittke and Chao's curve. The reason can be understood by the consideration of Fig. 1b, which shows the bubble surface temperature versus time for the three cases of Fig. 1a. Wittke and Chao assume the surface temperature to be at saturation for all times, while we allow it to change in response to the thermo-fluid-dynamics of the process. Although Wittke and Chao's approximation is seen to be justified over most of the collapse history, our results show that it is not so in the early stages of the process. At first, the surface temperature drops very fast due to a strong conductive heat loss, which causes a rapid condensation and a relatively fast collapse. As this fast collapse progresses, the latent heat released by the condensation raises the surface temperature, and with it the vapor pressure, so much that the direction of the radial motion is temporarily reversed. Soon the surface cools again, however, and the inward motion resumes,

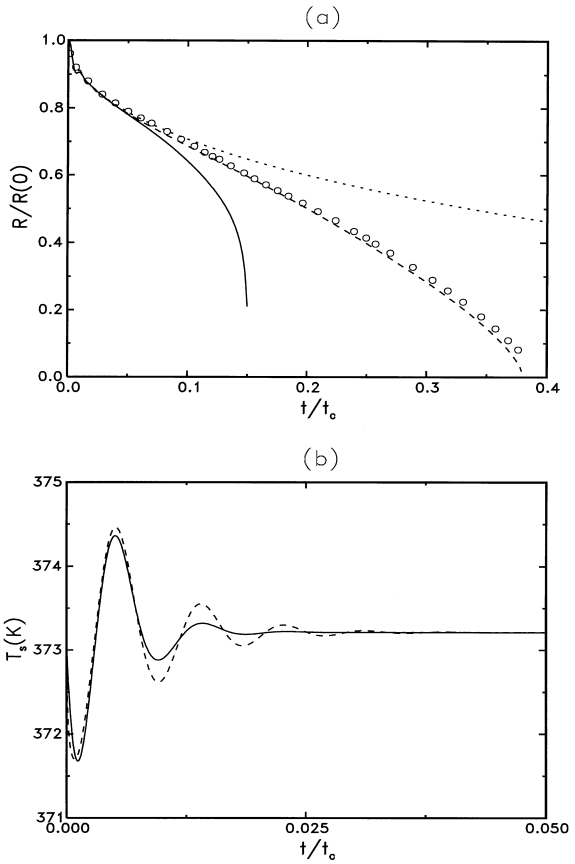

Fig. 1. Panel a shows the collapse of a 1 mm-radius bubble in water at a constant pressure of 1 atm for a subcooling of 3.35 K ($Ja = 10$). The dotted line is for a stationary bubble, the dashed line for a constant translational velocity of 0.127 m/s ($Pe = 1495$, $We = 0.293$), and the solid line for an initial translational velocity of 0.127 m/s adjusted according to Eq. (11) at later times; the circles are the numerical results of Wittke and Chao [4] for the constant velocity case. The time scale t_c, defined in Eq. (5), equals 46.2 ms. Panel b shows the bubble surface temperature for the three cases. At $t = 0$, the bubble surface is at the saturation temperature, while $T = T_\infty$ elsewhere.

this time more slowly. As a consequence, the latent heat can be removed from the surface sufficiently rapidly to maintain the collapse monotonic.

Figs. 2 and 3 are two other examples corresponding to different parameter values. For Fig. 2, $Pe = 2355$, $Ja = 29.9$ which, in water at 1 atm, would correspond to $R(0) = 1$ mm, a subcooling of 10 K, a velocity of 0.2 m/s, and $t_c = 5.19$ ms. In Fig. 3, $Pe = 1236$, $Ja = 29.9$ which, again in water at 1 atm, would correspond to $R(0) = 0.35$ mm, a subcooling of 10 K, a velocity of 0.3 m/s, and $t_c = 0.635$ ms.

The non-monotonic nature of the collapse is more evident here. Again, in the initial stages, the collapse is relatively strong and heat cannot be removed from the bubble surface fast enough to keep up with the latent heat deposited by the condensing vapor. Fig. 3b shows the radial distribution of the liquid temperature along different directions from the wake ($\theta = 0$) to the front stagnation point ($\theta = \pi$). This picture of the temperature field is taken at the instant $t/t_c = 0.2$ marked by a black circle in Fig. 3a, i.e. shortly after the first minimum of the radius. The region of heated liquid ahead of the bubble is very thin, as expected. The thermal wake extends much farther with a non-monotonic temperature distribution due to the high surface tempera-

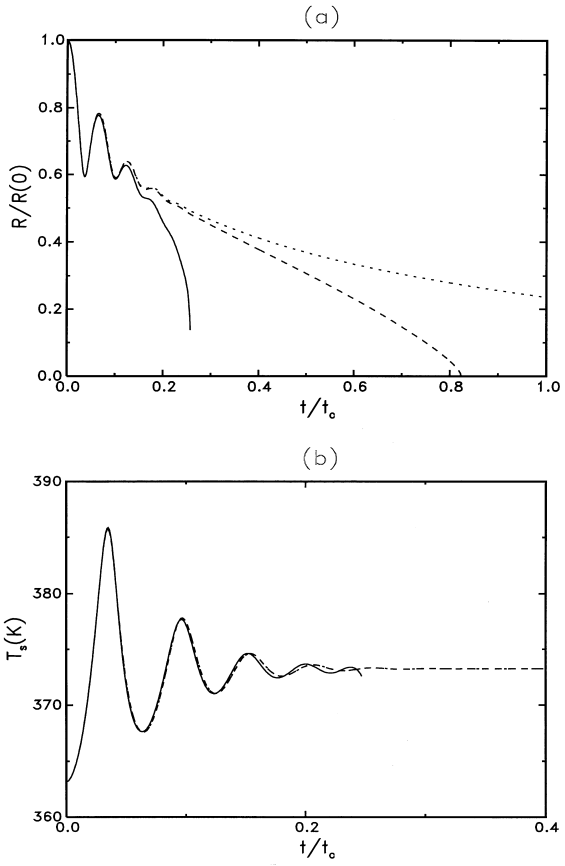

Fig. 2. Panel a shows the collapse of a 1 mm-radius bubble in water at a constant pressure of 1 atm for a subcooling of 10 K ($Ja = 29.9$). The dotted line is for a stationary bubble, the dashed line for a constant translational velocity of 0.2 m/s ($Pe = 2355$, $We = 0.678$), and the solid line for an initial translational velocity of 0.2 m/s adjusted according to Eq. (11) at later times; the time scale t_c, defined in Eq. (5), equals 5.19 ms. Panel b shows the bubble surface temperature for the three cases. At $t = 0$, the bubble surface is at the undisturbed liquid temperature T_∞.

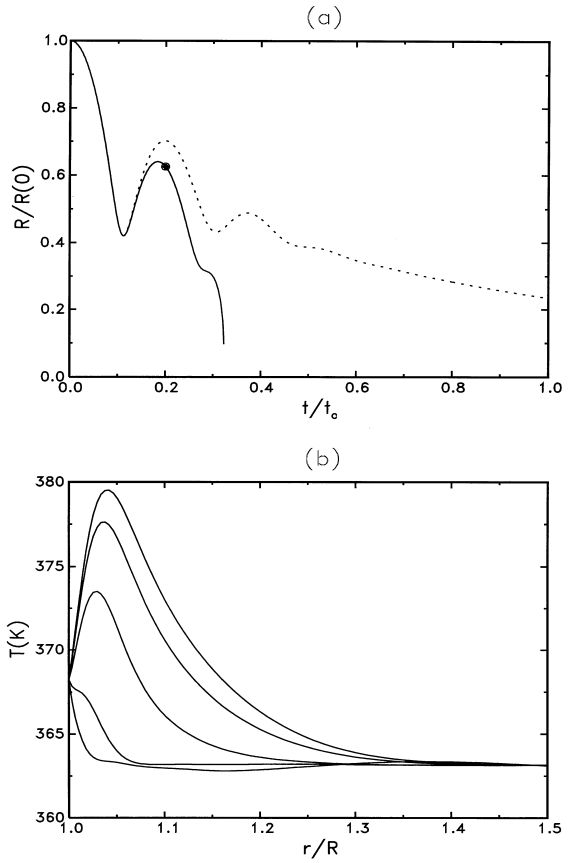

Fig. 3. Panel a shows the collapse of a 0.35 mm-radius bubble in water at a constant pressure of 1 atm for a subcooling of 10 K ($Ja = 29.9$). The solid line is for an initial translational velocity of 0.3 m/s ($Pe(0) = 1236$, $We(0) = 0.534$) adjusted according to Eq. (11) at later times, while the dotted line is for a stationary bubble; the time scale t_c, defined in Eq. (5), equals 0.635 ms. At $t = 0$, the bubble surface is at the undisturbed liquid temperature T_∞. Panel b shows the radial temperature distribution around the bubble in different directions with, in ascending order, $\theta = 180, 60, 30, 15$, and 0°; $\theta = 180^\circ$ points ahead of the bubble where $\theta = 0^\circ$ is along the line of symmetry of the thermal wake. This picture of the temperature field is taken at the instant $t/t_c = 0.2$ marked by a black circle in panel a.

ture around the time of the preceding radius minimum around $t/t_c \simeq 0.113$.

Although qualitative experimental evidence for this non-monotonic mode of collapse is well established (see, e.g., Refs. [3,10]), it should be noted that its details are strongly dependent on the liquid temperature field surrounding the bubble at $t = 0$. If one assumes $T = T_\infty$ everywhere in the liquid, a very rapid initial condensation takes place, which is responsible for the non-monotonic collapse as explained before. Experimentally, this situation can only be approached by subjecting a bubble, in saturated conditions, to a step pressure change. Any other procedure would necessarily build up a temperature distribution around the bubble with a strong effect on the collapse history. As an example, we show in Fig. 4 the collapse for an initial liquid temperature distribution given, for $R \le r \le R + \delta$, by

$$T(r, 0) = T_\infty + (T_{sat} - T_\infty)\left(1 - \frac{r - R(0)}{\delta}\right)^2, \qquad (26)$$

while $T = T_\infty$ for $R + \delta \le r$. The lines are, in ascending order, for $\delta/R(0) = 0$, 0.1, and 0.5. This calculation simulates the collapse of a 1 mm-radius bubble in ethanol with a subcooling of 31.6 K, a constant relative velocity of 0.28 m/s at a pressure of 1 bar; the dimensionless parameters have values $Pe = 7113$, $Ja = 47.5$, $\mu/\rho_L D_L = 12.6$. The behavior for $\delta = 0$ is strikingly different from that of the other two cases (with the surface temperature actually becoming so large as to invalidate our approximation of a constant latent heat).

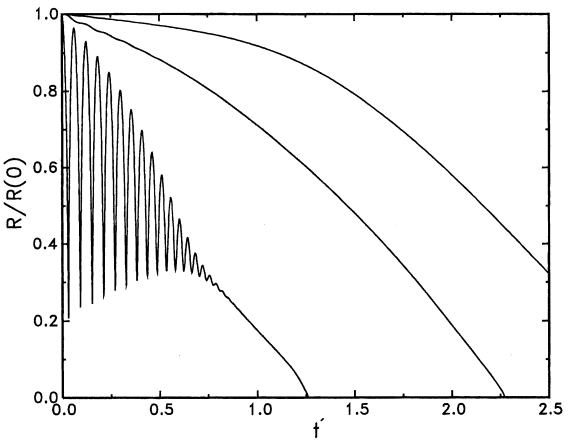

Fig. 4. Effect of the initial temperature distribution, given by Eq. (26), on the collapse of a 1 mm-radius bubble in ethanol with a subcooling of 31.6 K at 1 bar ($Ja = 47.5$) and a constant velocity of 0.28 m/s ($Pe = 7113$, $We = 2.94$). The lines are, in ascending order, for $\delta/R(0) = 0$, 0.1, and 0.5. Here, the dimensionless time is defined by $t' = Ja^2 D_L t/R(0)^2 = (\pi/4)(t/t_c)$ and $(4/\pi)t_c \simeq 3.18$ ms.

The results with $\delta/R(0) = 0.1$ approximately match the data of Chen as reported in Fig. 5 of Gumerov [9] and Gumerov's theory. To facilitate the comparison with Gumerov, here we non-dimensionalize the time by $t' = Ja^2 D_L t/R(0)^2 = (\pi/4)(t/t_c)$; numerically, $(4/\pi)t_c = 3.18$ ms. Clearly, an even better fit could be obtained by suitably adjusting the value of δ. This remark illustrates the difficulties that exist in attempting a comparison of theory and experiment. For example, Chen and Mayinger [10] generated bubbles by blowing (at an unspecified rate) saturated vapor from a nozzle into various degassed liquids. In these conditions, as the bubble grows, some vapor condenses and preheats the liquid so that, when the bubble detaches and starts condensing, the precise temperature distribution is not well known. A substantial heated layer around the bubble is quite evident in their pictures.

It is seen by comparing the solid lines with the dashed ones in Figs. 1 and 2 that, when the relative velocity is calculated according to Eq. (11) (with $dP/dx = 0$), the velocity increases with time so that the effect of convection is stronger and the collapse time reduced.

The momentum equation (11) is correct for a spherical bubble, which implies a sufficiently small value of the Weber number

$$We = \frac{\rho_L V_R^2 R(0)}{\sigma}. \qquad (27)$$

For high bubble velocities or in a fluid with a small surface tension, this condition will be violated and the bubble becomes distorted [31]. The effect is an increase of the added mass coefficient (see, e.g., Refs. [32,33]) which counters the decreasing volume and tends to limit the bubble acceleration. This is, for instance, the situation in some of the experiments of Chen and Mayinger with Refrigerant 113, which has a surface tension of only 13.7×10^{-3} N/m. Even in that case, however, a strong acceleration is quite evident near the end of the collapse (see their Fig. 9). For the cases of Figs. 1–3, the initial values of the Weber number are 0.293, 0.678, and 0.534 respectively, and, therefore, the spherical approximation is justified at least over a good portion of the collapse [10]. On the other hand, for the ethyl alcohol case of Fig. 4, the initial value of We is 2.94, and therefore, most likely, the bubble fairly distorted.

Let us now consider the behavior of a bubble carried in a region of increasing pressure. To model this situation, we use the relations (14)–(16) of Section 2. In all the cases, pressure far upstream is $P_\infty = 1$ atm (101.33 kPa); and at the initial instant, the bubble is released with the same local velocity as the liquid so that the relative velocity vanishes at $t = 0$.

Fig. 5 show the radius and position versus time for

a bubble with an initial radius $R(0) = 1$ mm with an upstream liquid velocity $U_\infty = 1$ m/s in saturated conditions ($T_\infty = 373.15$ K) for $\alpha = 0.15$. The dashed lines are for $\ell = 10$ mm, the solid lines for $\ell = 100$ mm, and the dotted line for a bubble stationary with respect to the liquid. The bubble is released from $x(0) = -\ell$, where the ambient pressure is 101.37 kPa, and therefore, the liquid slightly subcooled. When combined with the surface tension overpressure of 0.118 kPa, the effect is to promote the bubble collapse. The dotted line shows that in these conditions, the collapse would be very slow in the absence of a relative velocity. The situation for the bubble convected into the increasing pressure region is, however, quite different: the bubble acquires a negative velocity relative to the liquid, which is amplified due to conservation of impulse. As a consequence, the heat transfer at the bubble surface markedly increases and the collapse is far more rapid. As Fig. 5b shows, for $\ell = 10$ mm, this negative velocity becomes so large that the bubble actually ends up translating upstream. Due to the assumption of sphericity, in the present calculation, the relative velocity becomes unrealistically large in the late stages of the collapse. Nevertheless, the tendency for the bubble to be repelled by the increasing pressure and for the rate of collapse to be increased may be expected to be robust, realistic predictions. For the milder pressure gradient with $\ell = 100$ mm, both effects are less marked but nevertheless present.

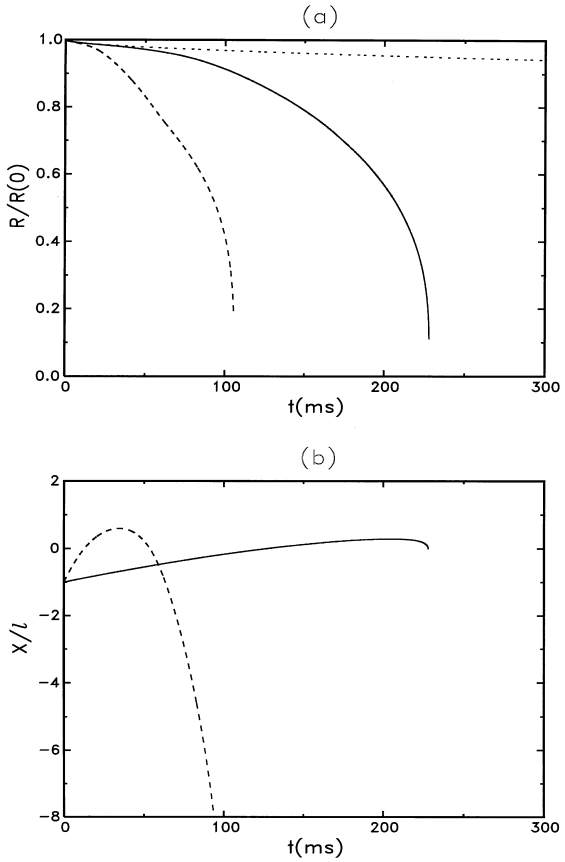

Fig. 5. Radius (panel a) and position (panel b) versus time for a 1 mm-radius bubble in water convected into a region of increasing pressure as given by Eqs. (14)–(16). The liquid temperature is 373.15 K and the upstream liquid velocity and pressure 1 m/s and 1 atm respectively; the parameter α of Eq. (14) has the value 0.15. The dashed lines are for $\ell = 10$ mm, the solid lines for $\ell = 100$ mm, and the dotted line for a bubble stationary with respect to the liquid. The bubble is released at $x(0) = -\ell$ with the same velocity as the liquid.

Results of the same calculations in the presence of a liquid subcooling of 1 K are shown in Fig. 6. Now the collapse is faster and the bubble has less time to pick up a relative velocity with respect to the liquid under the action of the adverse pressure gradient. As a consequence, the effect of the adverse pressure gradient is smaller.

When moving in the direction of an adverse pressure gradient, there is a curious situation that can be

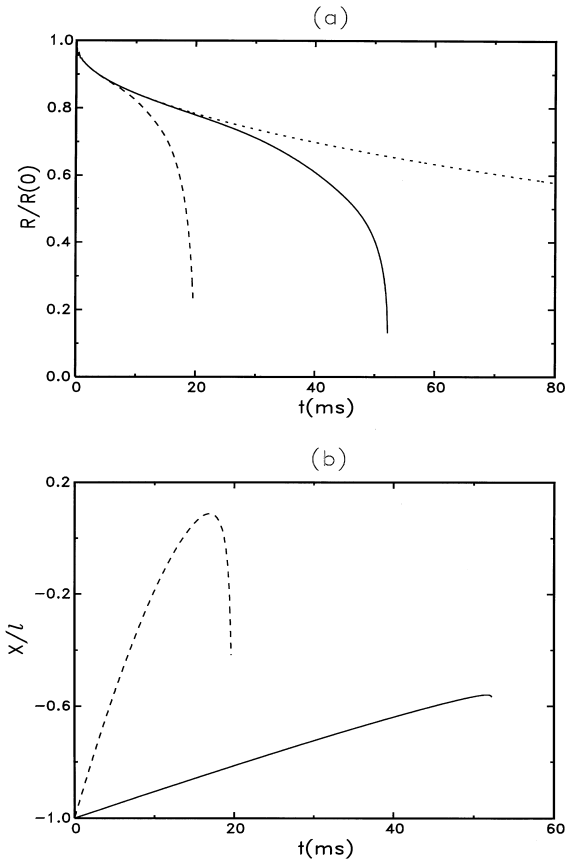

Fig. 6. As in Fig. 5, but with the liquid 1 K colder, $T_\infty = 372.15$ K.

encountered in which the bubble remains trapped at a fixed location in the flow. If U_B and dU_B/dt are set to zero in the bubble equation of motion (11), it is found that the equation will be satisfied provided that

$$\frac{1}{2}C_D U_L = -\frac{2}{3}R\frac{dU_L}{dx} - 2\frac{dR}{dt}. \tag{28}$$

Suppose the last term is unimportant. Then, since $U_L > 0$, for suitable $U_L(x)$, a balance is possible if $dU_L/dx < 0$, i.e. $dP/dx > 0$. A linearization of the equation about this fixed point reveals a damped oscillatory motion. If the bubble grows (but still with negligible U_B and dU_B/dt), the last term of Eq. (28) will be negative and can be so large as to change the sign of the entire right-hand side. In these conditions, no equilibrium exists and the bubble will be swept downstream with the flow. Conversely, if the bubble collapses, the right-hand side of Eq. (28) becomes more positive and the bubble has to drift in the direction of increasing U_L, i.e. upstream. It is evident, however, that it will be possible to satisfy the equation only up to a maximum collapse velocity. For larger collapse velocities, there is no equilibrium position and the bubble keeps moving upstream until the collapse is completed.

Examples of these behaviors are shown in Fig. 7 with $R(0) = 1$ mm, $\ell = 10$ mm, $\alpha = 0.15$, $U_\infty = 1$ m/s. Fig. 7a shows the radius versus time, while Fig. 7b shows the bubble position versus time with the lines corresponding, in ascending order, to $T_\infty = 373.18, 373.20, 373.22$, and 373.32 K. For the largest superheat, the bubble grows fast enough to be swept downstream. For $T_\infty = 373.22$, the bubble executes damped oscillations around a fixed position

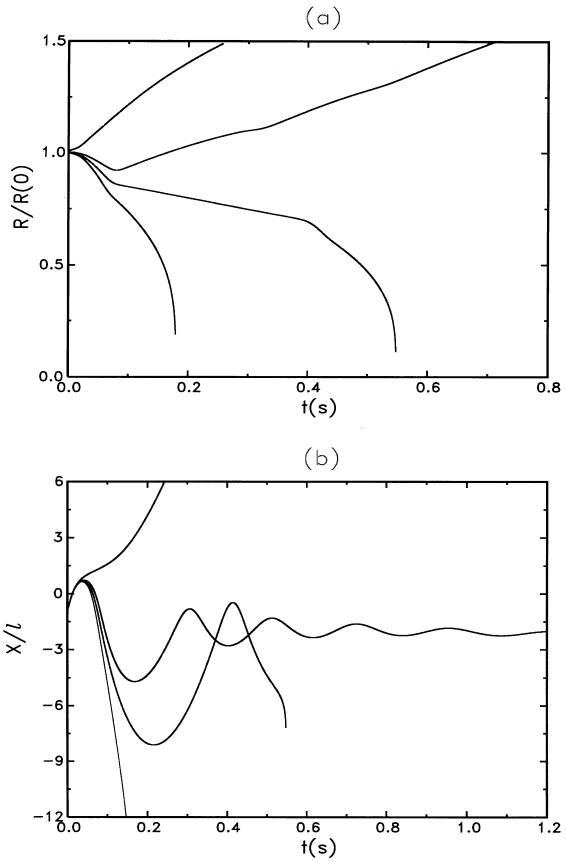

Fig. 7. Radius (panel a) and position (panel b) versus time for 1 mm-radius bubbles in water convected into a region of increasing pressure as given by Eq. (14)–(16), with upstream liquid velocity and pressure of 1 m/s and 1 atm, respectively; here $\ell = 10$ mm and $\alpha = 0.15$. The liquid temperature is, in ascending order, 373.18, 373.20, 373.22, and 373.32 K.

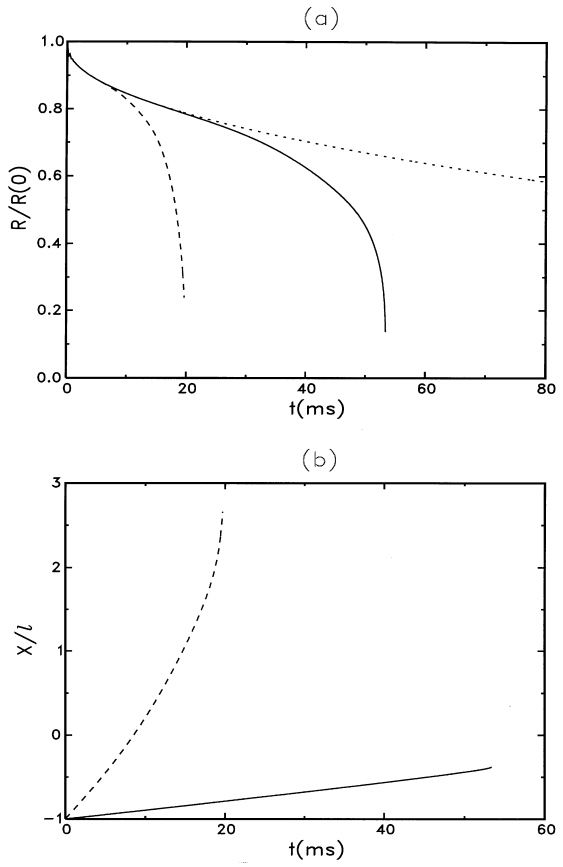

Fig. 8. Radius (panel a) and position (panel b) versus time for a 10 mm-radius bubble in water convected into a region of decreasing pressure as given by Eqs. (14)–(16). The liquid temperature is 372.15 K and the upstream liquid velocity and pressure 1 m/s and 1 atm, respectively; the parameter α of Eq. (14) has the value -0.15. The dashed lines are for $\ell = 10$ mm, the solid lines for $\ell = 100$ mm, and the dotted line for a bubble stationary with respect to the liquid. The bubble is released at $x(0) = -\ell$ with the same velocity as the liquid.

while growing slowly. Cooling the liquid by 0.02 K, is sufficient to cause the bubble to collapse while executing translational oscillations. A further decrease of the liquid temperature by another 0.02 K causes a collapse with the bubble ending up monotonically translating upstream. As illustrated in this example, the limit on $\mathrm{d}R/\mathrm{d}t$ for equilibrium to be possible is quite stringent and can only be satisfied for very small superheats.

In a real situation, where the flow is three-dimensional and the bubble is allowed to move laterally, the quasi-equilibrium situation just discussed would probably not be easy to observe. The fact, however, remains that an adverse pressure gradient tends to repel the bubble, and that the effectiveness of this repulsion is increased by condensation and decreased by growth.

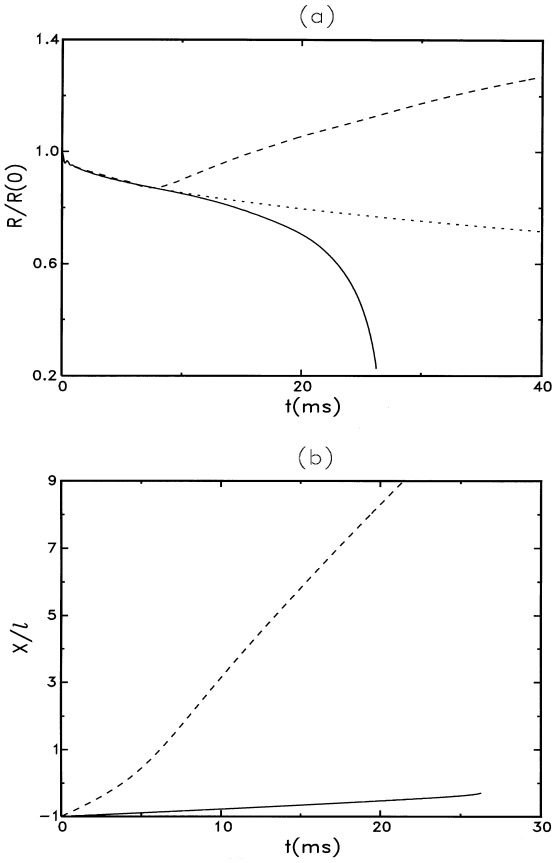

Fig. 9. Radius (panel a) and position (panel b) versus time for a 1 mm-radius bubble in water convected into a region of decreasing pressure as given by Eqs. (14)–(16). The liquid temperature is 372.15 K and the upstream liquid velocity and pressure 2 m/s and 1 atm, respectively; the parameter α of Eq. (14) has the value -0.3. The dashed lines are for $\ell = 10$ mm, the solid lines for $\ell = 100$ mm, and the dotted line for a bubble stationary with respect to the liquid. The bubble is released at $x(0) = -\ell$ with the same velocity as the liquid.

A contracting nozzle is considered in Figs. 8 and 9. Fig. 8a and b are for an initial radius $R(0) = 1$ mm in an upstream velocity $U_\infty = 1$ m/s in liquid subcooled by 1 K, with $\alpha = -0.15$. The dashed lines are for $\ell =$ 10 mm and the solid lines for $\ell = 100$ mm; the dotted line is for no relative motion as before. The favorable pressure gradient causes the relative velocity to be positive, so that the bubble leads the liquid. The position versus time shown in Fig. 8b indicates a nearly constant velocity in the early stages, where the bubble is essentially convected with the stream, followed by a strong acceleration as the relative velocity is amplified by the radius decrease.

The bubble response can be very different with a stronger favorable pressure gradient, the effects of which are shown in Fig. 9 for $R(0) = 1$ mm, in liquid subcooled by 1 K, but now with $U_\infty = 2$ m/s and $\alpha =$ -0.3. With $L = 100$ mm (solid lines), the bubble response is similar to that of the previous case. However, if the pressure gradient is stronger ($\ell = 10$ mm, dashed lines), the liquid becomes saturated at $x/\ell = 1.06$ and is superheated further downstream. Thus, the bubble starts collapsing upstream of $x/\ell = 1.06$ but, as the ambient liquid becomes supersaturated, the collapse is reversed and it begins to grow. Eq. (11) shows that, in this case, there is a tendency for the relative velocity to decrease and indeed Fig. 9b shows the bubble velocity ending up close to the downstream liquid $U_\infty(1 - \alpha)/(1 + \alpha) \simeq 3.71$ m/s.

5. Conclusions

We have examined the behavior of a vapor bubble immersed in a liquid flow in which velocity and pressure are spatially non-uniform. Because of the density difference between liquid and vapor, the pressure gradient causes the bubble to acquire a relative velocity with respect to the liquid with significant effects on heat transfer and radial dynamics. Due to the tendency of the system to conserve impulse, this relative velocity is amplified when the bubble collapses and reduced when it expands. As a consequence, the bubble's tendency to avoid high pressures and move toward low pressures is magnified in the former case and reduced in the latter.

In spite of several idealizations (inviscid flow, spherical bubble), the tendencies elucidated by the model may be expected to be qualitatively robust and could be of practical value for the management of vapor bubbles in microgravity conditions and other situations. A bubble that would only collapse slowly at rest with respect to the liquid, can be made to condense much faster by inducing a relative velocity by means of a pressure gradient. For example, flow through an expansion downstream of a boiling region

may significantly decrease the quality of a two-phase liquid–vapor mixture.

Acknowledgements

The authors express their gratitude to NASA for supporting this study under grant NAG3-1924.

References

[1] E. Ruckenstein, On heat transfer between vapour bubbles in motion and the boiling liquid from which they are generated, Chem. Eng. Sci 10 (1959) 22–30.
[2] R. Darby, The dynamics of vapour bubbles in nucleate boiling, Chem. Eng. Sci 19 (1964) 39–49.
[3] L.W. Florschuetz, B.T. Chao, On the mechanics of vapor bubble collapse, J. Heat Transfer 87 (1965) 209–220.
[4] D.D. Wittke, B.T. Chao, Collapse of vapor bubbles with translatory motion, J. Heat Transfer 89 (1967) 17–24.
[5] L.W. Florschuetz, C.L. Henry, A. Rashid Khan, Growth rates of free vapor bubbles in liquids at uniform superheats under normal and zero gravity conditions, Int. J. Heat Mass Transfer 12 (1969) 1465–1489.
[6] E. Ruckenstein, J. Davis, The effects of bubble translation on vapor bubble growth in a superheated liquid, Int. J. Heat Mass Transfer 14 (1971) 939–952.
[7] D. Moalem, S. Sideman, The effect of motion on bubble collapse, Int. J. Heat Mass Transfer 16 (1973) 2321–2329.
[8] N.A. Zolovkin, N.D. Negmatov, N.S. Khabeev, Heat and mass transfer of an individual vapor bubble in translational flow of an unbounded liquid volume, Fluid Dynamics 29 (1994) 386–391.
[9] N.A. Gumerov, The heat and mass transfer of a vapor bubble with translatory motion at high Nusselt numbers, Int. J. Multiphase Flow 22 (1996) 259–272.
[10] Y.M. Chen, F. Mayinger, Measurement of heat transfer at the phase interface of condensing bubbles, Int. J. Multiphase Flow 18 (1992) 877–890.
[11] D. Legendre, J. Bore, J. Magnaudet, Thermal and dynamic evolution of a spherical bubble moving steadily in a superheated or subcooled liquid, Phys. Fluids 10 (1998) 1256–1272.
[12] S. Gopalakrishna, N. Lior, Analysis of bubble translation during transient flash evaporation, Int. J. Heat Mass Transfer 35 (1992) 1753–1761.
[13] J.S. Ervin, H. Merte Jr, R.B. Keller, K. Kirk, Transient pool boiling in microgravity, Int. J. Heat Mass Transfer 35 (1992) 659–674.
[14] J.F. Klausner, R. Mei, D.M. Bernhard, L.Z. Zeng, Vapour bubble departure in forced convection boiling, Int. J. Heat Mass Transfer 36 (1993) 651–662.
[15] G.E. Thorncroft, J.F. Klausner, R. Mei, An experimental investigation of bubble growth and detachment in vertical upflow and downflow boiling, Int. J. Heat Mass Transfer 41 (1998) 3857–3871.
[16] T.B. Benjamin, A.T. Ellis, The collapse of cavitation bubbles and the pressures thereby produced against solid boundaries, Philos. Trans. R. Soc. London A260 (1966) 221–240.
[17] J.R. Blake, D.C. Gibson, Cavitation bubbles near boundaries, Ann. Rev. Fluid Mech 19 (1987) 99–123.
[18] A. Biesheuvel, L. van Wijngaarden, Two-phase flow equations for a dilute dispersion of gas bubbles in liquid, J. Fluid Mech 148 (1984) 301–318.
[19] D.Z. Zhang, A. Prosperetti, Ensemble phase-averaged equations for bubbly flows, Phys. Fluids 6 (1994) 2956–2970.
[20] A. Prosperetti, The thermal behaviour of oscillating gas bubbles, J. Fluid Mech 222 (1991) 587–616.
[21] D.A. Labuntsov, A.P. Kryukov, Analysis of intensive evaporation and condensation, Int. J. Heat Mass Transfer 22 (1979) 989–1002.
[22] Y. Hao, A. Prosperetti, The dynamics of vapor bubbles in acoustic pressure fields, Phys. Fluids 11 (1999) 2008–2019.
[23] L. van Wijngaarden, On the motion of gas bubbles in a perfect fluid, Arch. Mech 34 (1982) 343–349.
[24] H.N. Oğuz, A. Prosperetti, A generalization of the impulse and virial theorems with an application to bubble oscillations, J. Fluid Mech 218 (1990) 143–162.
[25] D.Z. Zhang, A. Prosperetti, Averaged equations for inviscid disperse two-phase flow, J. Fluid Mech 267 (1994) 185–219.
[26] J. Magnaudet, D. Legendre, The viscous drag on a spherical bubble with a time-dependent radius, Phys. Fluids 10 (1998) 550–554.
[27] A. Prosperetti, A.V. Jones, Pressure forces in disperse two-phase flows, Int. J. Multiphase Flow 10 (1984) 425–440.
[28] D.W. Moore, The boundary layer on a spherical gas bubble, J. Fluid Mech 16 (1963) 161–176.
[29] V.G. Levich, Physicochemical Hydrodynamics, Prentice-Hall, Englewood Cliffs, NJ, 1962 (Chapter 8).
[30] I.S. Kang, L.G. Leal, The drag coefficient for a spherical bubble in a uniform streaming flow, Phys. Fluids 31 (1988) 233–237.
[31] D.W. Moore, The velocity of rise of distorted gas bubbles in a liquid of small viscosity, J. Fluid Mech 23 (1965) 749–766.
[32] L.M. Milne-Thomson, Theoretical Hydrodynamics, 4th ed., Macmillan, New York, 1960.
[33] L. Noordzij, L. van Wijngaarden, Relaxation effects, caused by relative motion, on shock waves in gas-bubble/liquid mixtures, J. Fluid Mech 66 (1974) 115–143.